

# Cross-calibration of MODIS-A and -T using an intermediary geostationary sensor

Jing Tan, Robert Frouin, SIO/UCSD, La Jolla, California, USA

Hiroshi Murakami, JAXA, Tsukuba, Japan

## 1. Introduction

-Radiometric cross-calibration of optical (e.g., ocean-color) instruments, is an important activity to ensure product consistency and generate climate data records.

-It can be easily defined as viewing the same radiance at the same time, but it is much more difficult to achieve during in flight operations of different sensors on different orbits.

-Apart from viewing the Moon, one has to rely on measuring the solar radiation reflected by the Earth-atmosphere system at the same time and location because of its time variability.

-The Earth-atmosphere system has generally some bidirectional reflectance function that requires observing under the same solar and viewing geometry (i.e., same line of sight).

-If the spectral bands of the channels to be compared do not have the same or close definition, some empirical transformation has to be applied to make the comparison thus the cross-calibration.

## 2. Methodology

-The methodology utilizes AHI onboard geostationary satellite Hiwamari-8, which acts as an intermediary between the polar-orbiting sensors to calibrate (e.g., MODIS-A and MODIS-T). Level 1b MODIS and AHI TOA reflectance data (after vicarious calibration, i.e., SVC) were used.

-Consider the cross-calibration of two polar-orbiting sensors and assume for simplicity that polar-orbiting and geostationary sensors observe at exactly the same time ( $t$  or  $t'$ ). The cross-calibration coefficients between each polar-orbiting sensor and the geostationary sensor,  $A_{1i}$  and  $A_{2j}$ , can be written:

$$A_{1i} = \rho_{ref}(t) / f_{1i}[\rho_{1i}(t)]$$

$$A_{2j} = \rho_{ref}(t') / f_{2j}[\rho_{2j}(t')]$$

where  $f_{1i}$  and  $f_{2j}$  are empirical functions that relate  $\rho_{1i}$  and  $\rho_{2j}$  to  $\rho_{ref}$ . These functions are determined theoretically, from simulations for realistic environment and geometry conditions.

-If the two sensors are perfectly inter-calibrated,  $A_{1i}$  is equal to  $A_{2j}$ . Differences between  $A_{1i}$  and  $A_{2j}$ , on the other hand, will indicate that the calibration of the two sensors is not consistent and, therefore, needs to be adjusted accordingly.

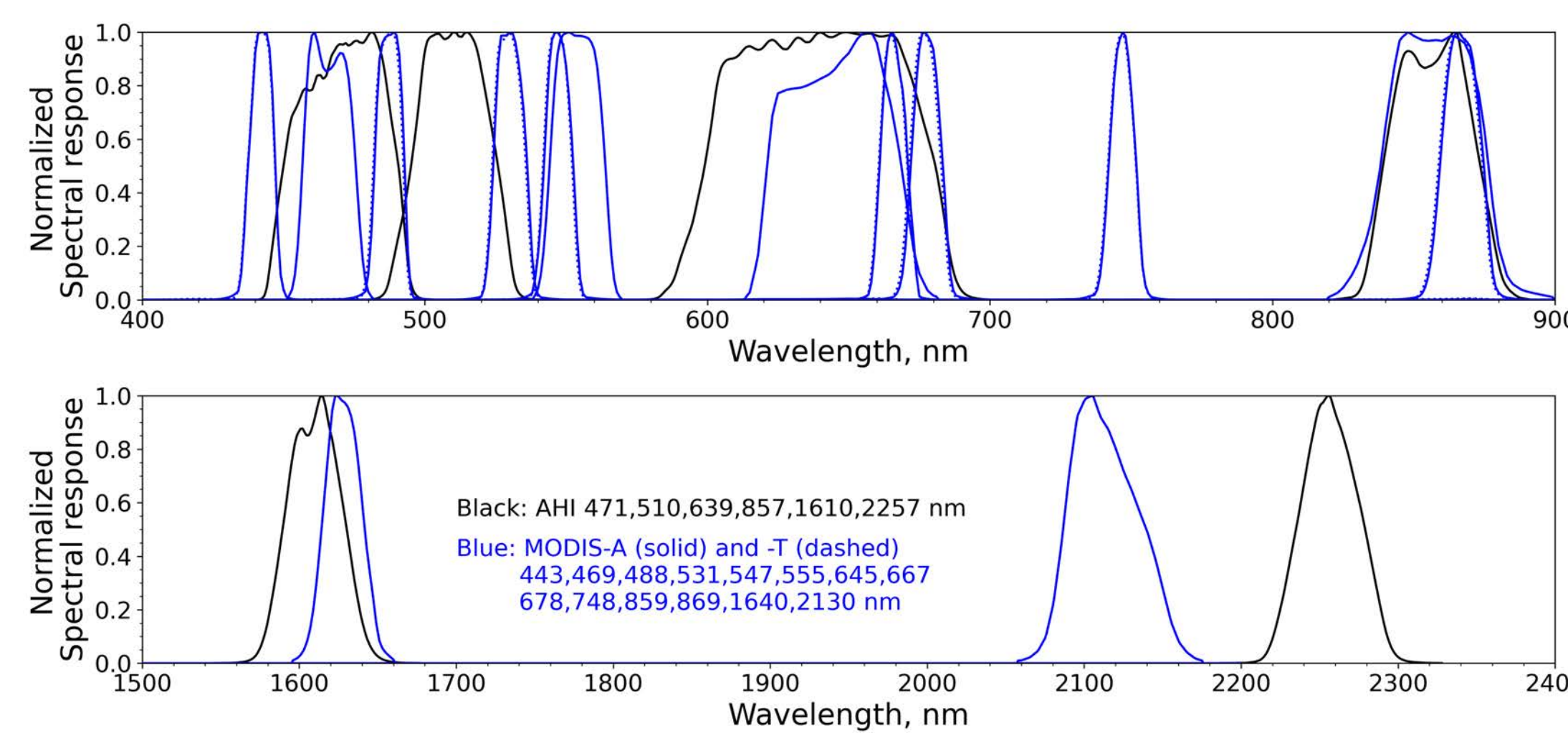
-Depending on the spectral band, the  $\rho_{ref}$  measurements may not be well correlated to  $\rho_1$  and  $\rho_2$  measurements in a single spectral band, but to measurements in several spectral bands. The formalism remains the same, but we now have:

$$A_{1M} = \rho_{ref}(t) / f_{1M}[\rho_{1i}(t), i = 1, 2, \dots, M]$$

$$A_{2N} = \rho_{ref}(t') / f_{2N}[\rho_{2j}(t'), j = 1, 2, \dots, N]$$

where the empirical functions  $f_{1M}$  and  $f_{2N}$  now relate  $\rho_{ref}$  to a combination of measurements  $\rho_{1i}$  in  $M$  spectral bands and  $\rho_{2j}$  in  $N$  spectral bands.

## 3. Spectral band matching



A list of the combinations of SGLI, MODIS-A, and -T bands used for estimating reflectance in AHI bands.

AHI bands (nm)	MODIS-A bands (nm)	MODIS-T bands (nm)
471	443&469, 443&488, 469&488, 469	443&469, 443&488, 469&488, 469
510	469&531, 469&547, 469&555, 488&531, 488&547, 488&555	469&531, 469&547, 469&555, 488&531, 488&547, 488&555
639	645, 667, 678	645, 667, 678
857	859, 869	859, 869
1610	1640	1640
2257	2130	2130

Normalized spectral response of AHI (black), MODIS-A (blue solid), and MODIS-T (blue dashed) bands.

Radiative transfer simulations using the Second Simulation of a Satellite Signal in the Solar Spectrum Vector (6SV) code were used to simulate AHI, MODIS-A and -T TOA reflectance for a wide range of aerosols and marine reflectance conditions. Only Case 1 waters were considered to avoid the high variability of coastal turbid waters, i.e., the matching corresponds to situations encountered in open waters, where the coincidences will be selected.

AHI Bands	MODIS Bands	MODIS-A				MODIS-T			
		$a_{1s}$ , $a_{2s}$ or $a_1$	$a_0$	RMSD	$a_{1s}$ , $a_{2s}$ or $a_1$	$a_0$	RMSD		
471	443,	-0.14561,	-0.00039	0.00027	-0.14500,	-0.00039	0.00027		
	469,	1.14226	(0.2%)	1.14165	(0.2%)				
	433,	0.35026,	-0.00062	0.00042	0.34054,	-0.00063	0.00042		
	488,	0.65026	(0.3%)	0.66387	(0.3%)				
	469,	0.80135,	0.00014	0.00008	0.79514,	0.00013	0.00008		
	488,	0.19783	(0.1%)	0.20406	(0.1%)				
510	469,	0.99300	-0.00190	0.00094	0.99300	-0.00190	0.00094		
	488,	0.43529,	0.00052	0.42483,	0.00052	0.42483,	0.00032		
	531,	0.56452	(0.4%)	0.57500	(0.3%)				
	488,	0.56559,	-0.00015	0.00063	0.55650,	-0.00019	0.00061		
	547,	0.43411	(0.6%)	0.44324	(0.5%)				
	488,	0.60001,	-0.00018	0.00071	0.59309,	-0.00023	0.00069		
	555,	0.39895	(0.6%)	0.40586	(0.6%)				
	469,	0.28057,	-0.00055	0.00034	0.27681,	-0.00036	0.00033		
	531,	0.72411	(0.3%)	0.72222	(0.3%)				
	469,	0.39508,	-0.00051	0.00056	0.39309,	-0.00051	0.00056		
547,	0.60358	(0.5%)	0.60560	(0.5%)					
469,	0.42883,	-0.00057	0.00066	0.42883,	-0.00057	0.00066			
555,	0.56868	(0.6%)	0.56868	(0.6%)					

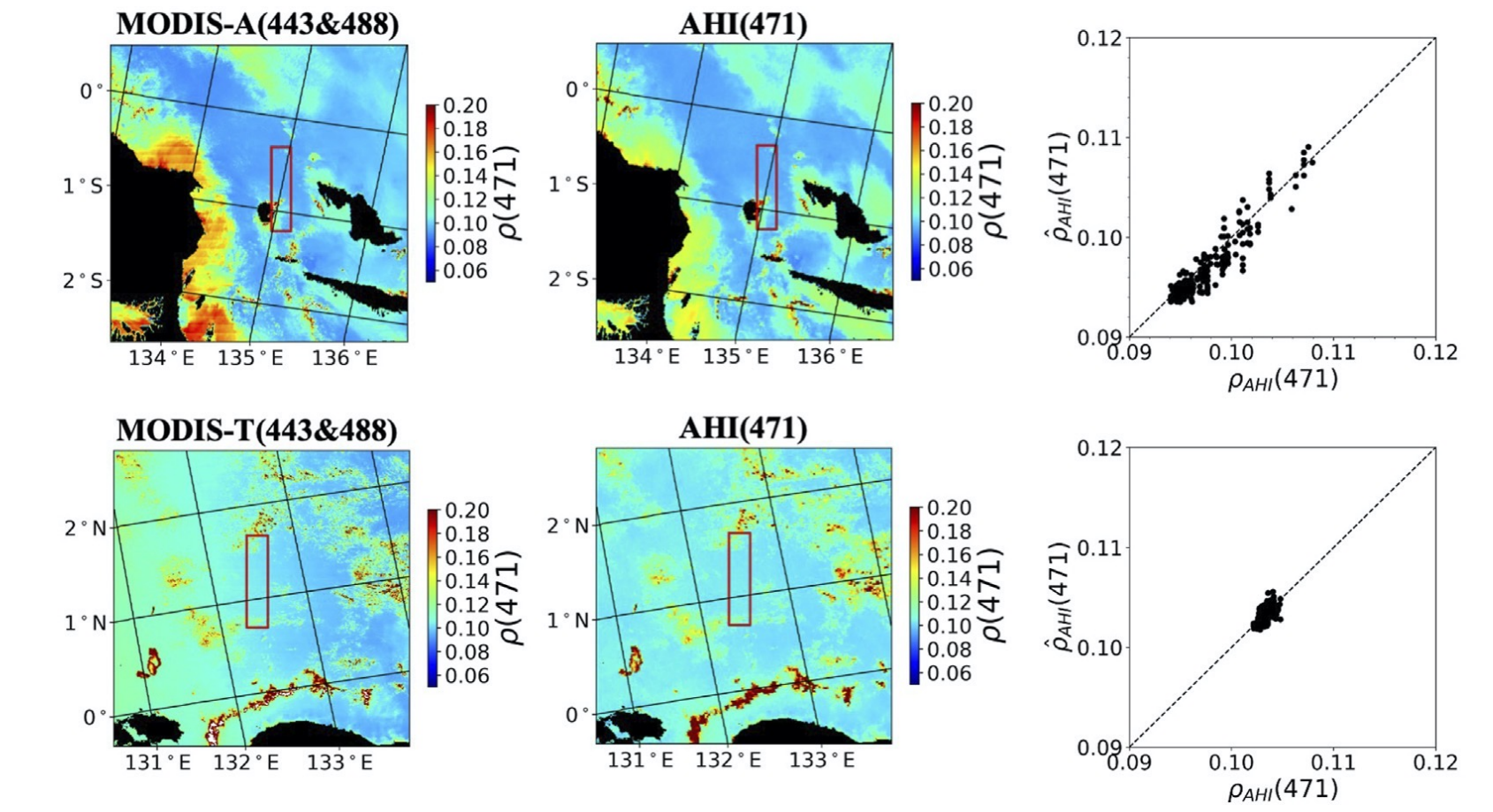
The relations and corresponding RMSD for MODIS-A, and -T band combinations to generate equivalent AHI bands, obtained using 6SV simulations with VZA  $\leq 45^\circ$ , SZA  $\leq 60^\circ$ , and no gaseous absorption. TOA reflectance (denoted as  $p$ ) at each AHI band can be generated using  $a_0 + a_1 * p_{s1} + a_2 * p_{s2}$  or  $a_0 + a_1 * p_{sj}$ , where subscript  $s$  represents MODIS-A, or MODIS-T, and  $i, j$  represents band  $i$  and  $j$ .

AHI Bands	MODIS Bands	MODIS-A				MODIS-T			
		$a_{1s}$ , $a_{2s}$ or $a_1$	$a_0$	RMSD	$a_{1s}$ , $a_{2s}$ or $a_1$	$a_0$	RMSD		
639	645	0.99122	0.00227	0.00059	0.99122	0.00227	0.00059		
	667	0.97076	0.00717	0.00190	0.97020	0.00729	0.00194		
	678	0.96150	0.00944	0.00252	0.96037	0.00953	0.00255		
857	859	1.00002	0.00001	0.00000	1.00002	0.00001	0.00000		
	869	0.99743	0.00062	0.00020	0.99745	0.00059	0.00019		
1610	1640	0.99001	0.00008	0.00004	0.99001	0.00008	0.00004		
2257	2130	0.89233	-0.00055	0.00058	0.89233	-0.00055	0.00058		

## 4. Geometry Coincidence

The observation time ( $t$ , GMT), geometry (solar zenith  $\theta_s$ , view zenith  $\theta_v$ , relative azimuth  $\phi$ , and scattering angle  $\theta$ ), latitude/longitude, and total number of collocated pixels ( $N$ ) for each sensor pair on the three different dates.

Sensors	Date	N	t	Lat/Lon	$\theta_s$	$\theta_v$	$\phi$	$\theta$
AHI/ MODIS-T	11 May 2018	684	01:30	0.7°-2.0°N, 132.1°-132.7°E	26.9°	8.7°	44.3°	157.7°-158.8°
	22 Jan 2019	257	01:30	0.5°-1.8°N, 132.3°-132.9°E	33.4°	10.7°	29.9°	153.8°-155.4°
	25 Jan 2020	619	01:30	0.5°-2.0°N, 132.2°-132.8°E	33.2°	10.9°	28.6°	154.1°-155.8°
AHI/ MODIS-A	11 May 2018	396	04:30	0°-1.5°S, 134.7°-135.3°E	30.1°	5.6°	128.0°	143.9°-145.5°
	25 Jan 2020	381	04:30	0°-1.5°S, 134.7°-135.3°E	27.4°	7.9°	139.7°	146.3°-148.0°



Concomitant MODIS-A/AHI (04:30 GMT top row), and MODIS-T/AHI (01:30 GMT, bottom row) imagery acquired on 25 January 2020. The AHI imagery of 471 nm was remapped to the MODIS latitude-longitude grid, and MODIS-A and -T at 443 and 488 nm were used to generate the equivalent AHI image at 471 nm. Red rectangles indicate where the coincident pixels occur. Land is masked as black. White indicates saturated pixels. The right panel show the scatter plots of equivalent versus measured AHI reflectance.

## 5. Cross-calibration Results

- Assume that the cross-calibration coefficients of sensors  $A/B$  and  $A/C$  at band  $i$  are expressed as  $R_{i(AB)} \pm \delta_{i(AB)}$  and  $R_{i(AC)} \pm \delta_{i(AC)}$ , the cross-calibration coefficient for  $C/B$  is then calculated as  $R_{i(CB)} = R_{i(AB)}/R_{i(AC)}$ , and the associated error as  $\delta_{i(CB)} = R_{i(AB)}/R_{i(AC)} \sqrt{(\delta_{i(AB)}/R_{i(AB)})^2 + (\delta_{i(AC)}/R_{i(AC)})^2}$

- Given that the cross-calibration coefficients of band  $i$  are from a distribution with mean  $\mu_i$  and variance  $\sigma_i^2$  and independent measurements are made at each day  $j$  with known error (i.e.,  $R_{i,j} \pm \delta_{i,j}$ ), the inverse-variance weighted average which minimizes the variance of the weighted average is used to represent  $\mu_i$ :  $\mu_i = \sum_{j=1}^n \omega_{i,j} R_{i,j}$

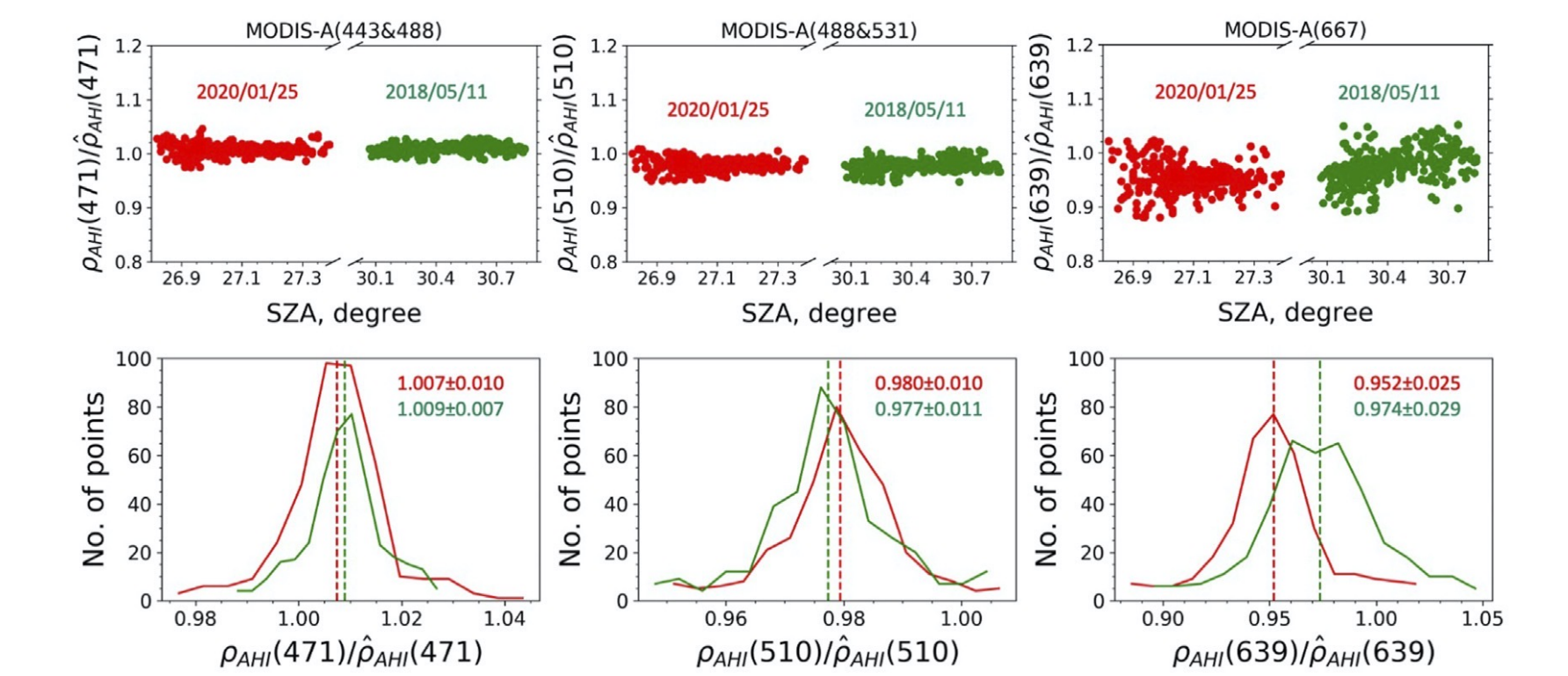
with the weights  $\omega_{i,j}$  expressed as:  $\omega_{i,j} = \frac{1/(\sigma_i^2 + \delta_{i,j}^2)}{\sum_{j=1}^n 1/(\sigma_i^2 + \delta_{i,j}^2)}$

and the uncertainty of  $\mu_i$  calculated as:  $\delta_{\mu_i} = \sqrt{\frac{1}{\sum_{j=1}^n 1/(\sigma_i^2 + \delta_{i,j}^2)}}$

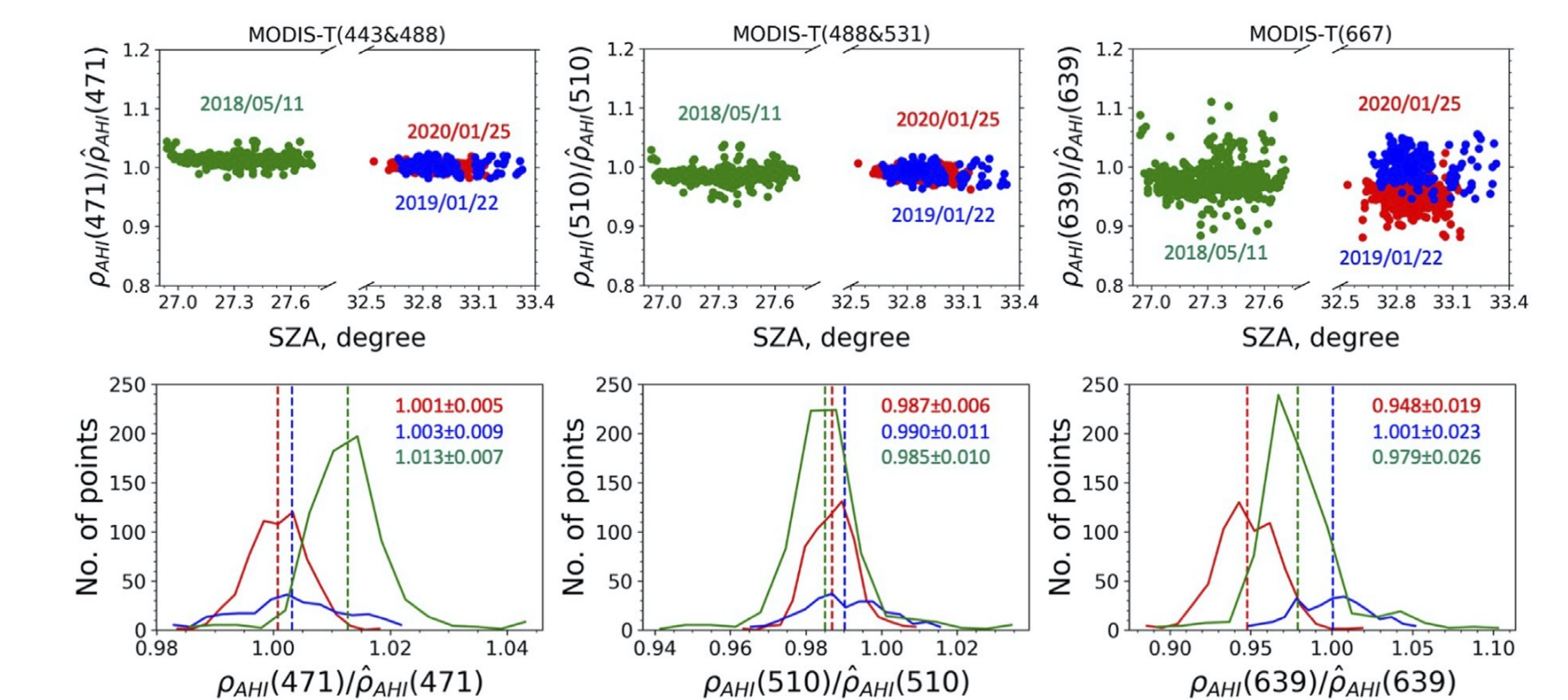
where  $n$  is the total number of days.

- When the number of samples (days) is sufficiently large, estimating  $\sigma_i$  and the weights  $\omega_{i,j}$  can be done iteratively.

- To overcome the lack of days in this study, the population standard deviation  $\sigma_i$  is estimated from reported uncertainties on vicarious gains. The uncertainty on the AHI calibration coefficients is not needed because they can be assumed constant when cross-calibrating AHI and each of the polar-orbiting sensors during the same day.



(Top) cross-calibration coefficients versus solar zenith angle, SZA, and (bottom) histograms of cross-calibration coefficients for AHI/MODIS-A at 471, 510, and 639 nm. Different colors represent different dates. Vertical lines indicate the means, whose values, together with standard deviations, are specified in the insets.



Same as above, but for the equivalent AHI at 471, 510, and 639 nm generated using MODIS-T 443&488 nm, 488&531 nm, and 667 nm.

The best estimate of cross-calibration coefficients  $A$  and associated uncertainties for MODIS-A/MODIS-T. The cross-calibration coefficients obtained for individual days are listed in parentheses.

Band combinations	AHI(471) 469	AHI(471) 443&488	AHI(471) 443&469	AHI(471) 469&488	AHI(510) 488&531	AHI(510) 488&547	AHI(510) 488&555
Cross-calibration coefficient A	(0.991, 0.984) 0.988±0.010	(1.004, 0.994) 0.999±0.006	(0.993, 0.988) 0.991±0.007	0.997, 0.991 0.994±0.009	(1.008, 1.008) 1.008±0.006	(1.004, 1.009) 1.007±0.006	(1.005, 1.010) 1.008±0.006

Band combinations	AHI(510) 469&531	AHI(510) 469&547	AHI(510) 469&555	AHI(639) 645	AHI(639) 667	AHI(639) 678
Cross-calibration coefficient A	(1.007, 1.005) 1.006±0.006	(0.999, 1.002) 1.000±0.006	(0.999, 1.005) 1.002±0.006	(1.002, 0.989) 0.995±0.007	(1.005, 0.996) 1.001±0.007	(1.006, 1.001) 1.004±0.007

## 6. Conclusions

-Using an intermediary sensor in geostationary orbit allows one to find numerous coincident measurements in space, time, and geometry over oceanic regions (signal level for ocean-color applications), an advantage over other cross-calibration techniques.

-MODIS-A and MODIS-T after SVC are well cross-calibrated in the bands of reference, with differences of about 1% from unity, generally within the uncertainties, for all band combinations.

-The method proposed in this study can be applied operationally, and to other optical sensors operating in polar orbit. It can also be performed prior to SVC, as this calibration may be considered as part of the atmospheric correction process.

-The cross-calibration coefficients obtained on each day is accurate (with small uncertainties), and the time series allows one to observe how the cross-calibration between polar orbiting sensors changes with time.

-The methodology has great potential in the future in view of new geostationary sensors, which will have improved performance and characteristics, allowing a more accurate and complete cross-calibration of polar-orbiting optical sensors. For example, cross-calibrating the new PACE mission with GLIMR.

**Acknowledgements:** This work was funded by JAXA under Contract 22RT000268 and NASA under Grant 80NSSC21K1661. The authors gratefully acknowledge the NASA OBP and JAXA EORC for generating, maintaining, and distributing the Level-1 satellite products used in the study.